

# Hudson River Flood Impact Decision Support System

## Version 2: Technical Information

**Hudson River Flooding Decision Support System Version 1**

Scenario Builder/Layer List

Print Tips Download Statistics Upload Your GIS Data Legend

Layer List >>

Build Your Flood and Inundation Scenario

Choose Area of Interest

County: Albany

Town: Albany

Select Flood Scenario

Sea Level: 72 inches

Return Period: 1000 year

Submit Filter Reset Filter

Impact Summary for Albany (fipskey: 3600101000)

Critical Infrastructure	Natural Resilience	Social Vulnerability
Total Damaged Buildings: 379		
Buildings with Substantial Damage: 35		
Building Loss: 265421000 (\$)		
Contents Loss: 671329000 (\$)		
Depreciated Building Loss: 864190000 (\$)		
Depreciated Contents Loss: 214792000 (\$)		
SPDES Wastewater: 6		
Bridges: 47		
Railroads: 34 (Linear Miles)		
Railroad Junctions: 1		
Boat Launches: 1		
Bus Routes: 62 (Linear Miles)		
Bus Stations: 1		
Power Transmission Lines: 3 (Linear Miles)		
Police Stations: 1		
Schools: 1		
Places of Worship: 10		

Icon fill color indicates:

- Not in flood zone
- In flood zone
- No flood info

Icon shape indicates layer group, icon border color corresponds to layer-name color (for clickable layers within group). For complete layer information please see the Data Dictionary (pdf)

Hudson River Features

- Emergency Services
- Health Services
  - Nursing homes
  - Hospitals
- Water and Wastewater
  - SPDES Wastewater
  - Wells
  - Water Withdrawal Locations
  - Dams
- Energy Production
  - EIA power plants
- Transportation Infrastructure
- Institutions
  - Schools
  - Public libraries
  - Prisons
  - Places of worship
- Social Vulnerability
  - Social Vulnerability Index
  - Municipal SoVI
- Contextual Information
- Ecology
  - Forest Patches 2010
  - Important Animal Areas
  - Important Plants Area
  - Natural Estuarine Communities
  - Natural Riverine Communities
  - Natural Palustrine Communities
  - Natural Terrestrial Communities
  - NWI Wetlands
- Administrative
- Base maps

Legend

Icon fill color indicates:

- Not in flood zone
- In flood zone
- No flood info

Ecology

Flood Scenario

- Not Flooded
- 0m
- 12m
- Possible Flooding - Disconnected

Estuary Shoreline

Municipality

County

Full Study Area

Water and Wastewater

- SPDES Wastewater

Map Feedback

## Table of Contents

Project Summary.....	4
Flood Scenarios: Methods .....	5
Storm flood hazard assessment.....	5
Modeling.....	8
Sea level rise .....	9
Flooding from tides with sea level rise .....	10
Flood Scenarios: Results .....	11
Storm tides with sea level rise .....	11
Tides with sea level rise .....	13
Mapping.....	15
Social Vulnerability.....	16
Theoretical framework .....	16
Social Characteristics .....	16
Economic status.....	16
Isolation.....	17
Health.....	17
Variable selection.....	17
Indicator construction.....	17
Data cleaning .....	17
Data transformation and normalization .....	17
Data reduction .....	18
Output vulnerability dimensions .....	18
Aggregation.....	19
Impact Estimates.....	20
Critical Infrastructure.....	20
Natural Resilience Features .....	20
Social Vulnerability.....	21
Climate Smart Communities Flood Adaptation Guidance .....	21
Acknowledgements.....	23

References .....	24
Appendix 1. Detailed Methods and Model Validations .....	26
Storm flood modeling validations.....	26
Tidal flood assessment.....	27
Appendix 2. The Variable Framework of the Social Vulnerability Index. The codes used in the last column represent Census variables used for the analysis.....	29
Appendix 3. Dimensions of Social Vulnerability based on PCA - Block Group Level .....	35
Appendix 4. Dimensions of Social Vulnerability based on PCA - Municipal Level .....	38

## Project Summary

The data, maps, and information in the Hudson River Flood Impact Decision Support System version 1 illustrate the scale of potential flooding for tidally-affected shorelines of the Hudson River Valley and Westchester County under multiple sea level rise and storm scenarios to assist individual residents, communities, and municipal and regional planners.

This information is unique because it is based on “dynamic” water flow modeling that combines tides, storm surges, sea level rise, and tributary freshwater inputs to the Hudson (Orton et al., 2018; Orton et al., 2016). The flood zones for 5-year to 1000-year storm events are created using statistical analysis of data for a set of 881 storms representative of the various types of storms that could strike the region. The dynamic model is the same one that is used for the New York Harbor Observing and Prediction System (NYHOPS; <http://stevens.edu/nyhops>).

Our modeling and mapping methodology is motivated by prior research that shows that it is not appropriate to assume storm surge and rain act independently to cause independent flood events (Orton et al., 2012). The modeling demonstrates that it is inaccurate to assume that sea level rise uniformly increases storm-driven flood elevations at all locations (“static superposition”). This assumption is very good along the Hudson from Poughkeepsie southward, but in prior work we have shown that it leads to small low-biases in flood elevation estimates for Long Island Sound (Kemp et al., 2017) and here we show that it leads to large high-biases for areas further northward along the Hudson.

The sea level rise scenarios available within the tool range from 0 to 6 feet (0 to 1.83 m) above the base mean sea level of 1983-2001, a standard sea level used by the National Oceanic and Atmospheric Administration (NOAA). Current projections from the updated ClimAID report still show high uncertainty about future sea level rise. Projections for the year 2100 range from 1.25 to 6.25 feet (0.38 to 1.91 m), the 10<sup>th</sup> and the 90<sup>th</sup> percentile values, respectively. These apply to the Hudson River nearest New York City, but we note that numbers for the Hudson near the Troy dam are a few inches lower (Horton et al., 2015). The Sea Level Rise section of this report describes estimates of the year when we expect to see each of the sea levels highlighted in the web tool.

The flood events are modeled with NYHOPS in tidal waterways, but mapped out onto surrounding floodplains using a simplified “bathtub” methodology. Water level (also known as still water elevation) estimates produced by this modeling are subtracted from the New York State Department of Environmental Conservation’s (NYSDEC) 2011-2012 LIDAR-based land elevation dataset in order to produce flood depth estimates (Department of Commerce, 2011). The flood mapping procedure is described in more detail in the Mapping section of this report.

Each of the flood scenarios presented in the mapping tool are accompanied by a set of impact estimates. These are divided into three themes: critical infrastructure, social vulnerability, and natural resilience features. Critical infrastructure impacts are estimated at the municipal level and consist of loss estimates derived from the HAZUS-MH 2.2 Flood Model, as well as counts of affected facilities, landmarks, and physical features. The social vulnerability information is summarized at the municipal and block group levels and is derived from a social vulnerability index based on the 2010 US Census, and

American Community Survey (ACS) data. The information on natural resilience features is produced by calculating inundated and total land areas for several variables important for conservation and storm water amelioration. Each of these sets of impact estimates are described in more detail in the Impact Estimates section of this report.

## Flood Scenarios: Methods

Flood zones are mapped along the Hudson River and Westchester County's western Long Island Sound floodplains, accounting for storm surge, tides, rainfall flooding, and several scenarios of sea level rise in corresponding towns and municipalities. The user can choose from a range of flood events (by return period or for high tide only) and sea level rise scenarios. Tributary floodplains are not included in the modeling and mapping – the flood mapping is only for the tidally-affected shorelines and adjacent floodplains. Details on the statistical flood hazard assessment, dynamic water modeling, sea level rise, and tidal flood simulations are provided in four subsections below.

### Storm flood hazard assessment

A flood event return period (P) represents the expected average time between events; the inverse of return period (1/P) is the probability that a storm will occur in a given year. For example, the 100-year event is expected to have a 1/100 chance (or 1 percent chance) of happening each year. Because this is an *annual* probability, a “100-year event” does not mean that it will only occur once every 100 years. Although the probability is low, 100-year events have been known to occur twice in one year, or in back-to-back years.

The general statistical framework for the study requires four steps (Orton et al., 2018; Orton et al., 2016): (1) historical data review, (2) storm climatology construction, (3) flood modeling, and (4) statistical analysis. The process is repeated for each sea level scenario. Resulting data for each location describes the water level at each return period (or inversely, the probability of a given water level being reached).

The worst historical flood events at NYC (Battery), western Long Island Sound (Kings Point), and Albany have been a mixture of tropical cyclones (TCs), offshore extratropical cyclones (ETCs; e.g. Nor'easters), and inland wet extratropical cyclone floods (WETCs; e.g. freshets, rain-on-snow events) (**Figure 1**). These types of events are all accounted for in the flood hazard assessment by (a) performing model validation on the worst historical events in each category and (b) creating a climatology of the possible storms in each.

The ETC climatology illustrates 30 of the region's worst historical storm surge events, with wind and atmospheric pressure data created for a regional FEMA flood mapping study (FEMA, 2014) by Oceanweather Inc. Streamflow inputs to the Hudson are derived from historical data.

The WETC storm climatology was derived by ranking historical streamflows from 1931-2013 at Troy, New York, and choosing the top 41 events that have occurred in the “cool season,” December through May, avoiding tropical cyclone events. As with ETCs, streamflow inputs to the Hudson are derived from

historical data. Meteorological forcing (e.g. wind) is not imposed, as the streamflows dominate the water elevations for these storms and high-resolution meteorological data for the entire period is not available.

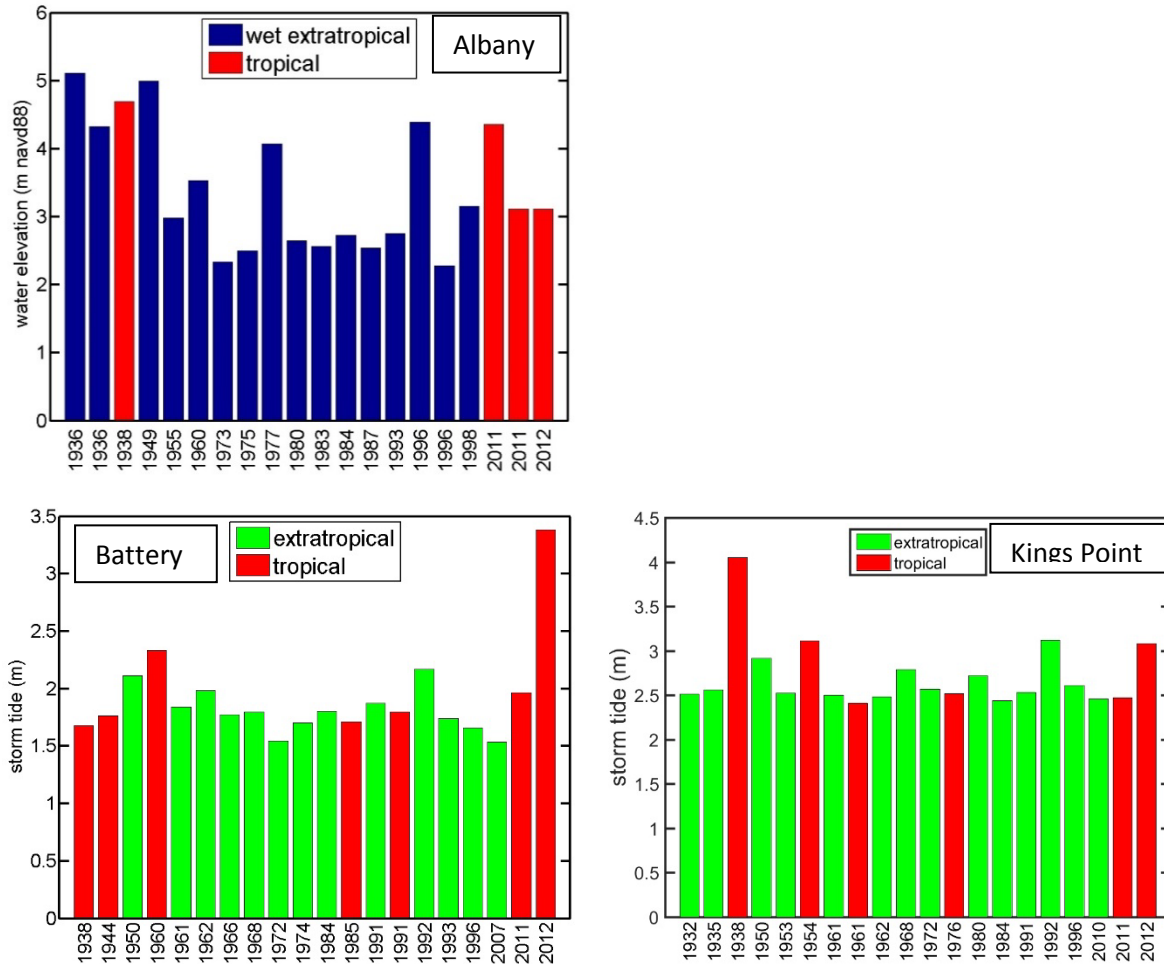


**Figure 1:** Historical top-20 flood events from 1931-2012 at Albany (top), New York City’s Battery Park (bottom left), and western Long Island Sound (bottom right). Tropical cyclones include tropical storms and hurricanes. Extratropical cyclones include nor’easters and other types of non-tropical storms.

For the TC climatology, a set of 637 synthetic TCs is created based on a statistical model (e.g., Hall & Yonekura, 2013) derived from the statistics of historical North Atlantic TCs (1900 - 2010). Sample storm tracks are shown in **Figure 2**, focusing on storms that led to roughly 100-year floods. We use simple parametric equations to represent each storm’s wind and pressure forcing for our ocean model (Orton et al., 2018; Orton et al., 2016). The modeling subsection below describes the methodology for modeling TC river streamflows.

Tides for these storm simulations are randomly selected from a time series of tides from 1900-2013, with one simulation with random tide for each TC, one for each WETC, and 50 simulations with random tides for each ETC, where tides are a larger proportion of the total water level. That is, the ETC storms are run 50 times each, once for each random tide scenario. Tides are included in the hydrodynamic model and imposed at the edge of the continental shelf, as in the NYHOPS forecasting system (Georgas & Blumberg, 2009).

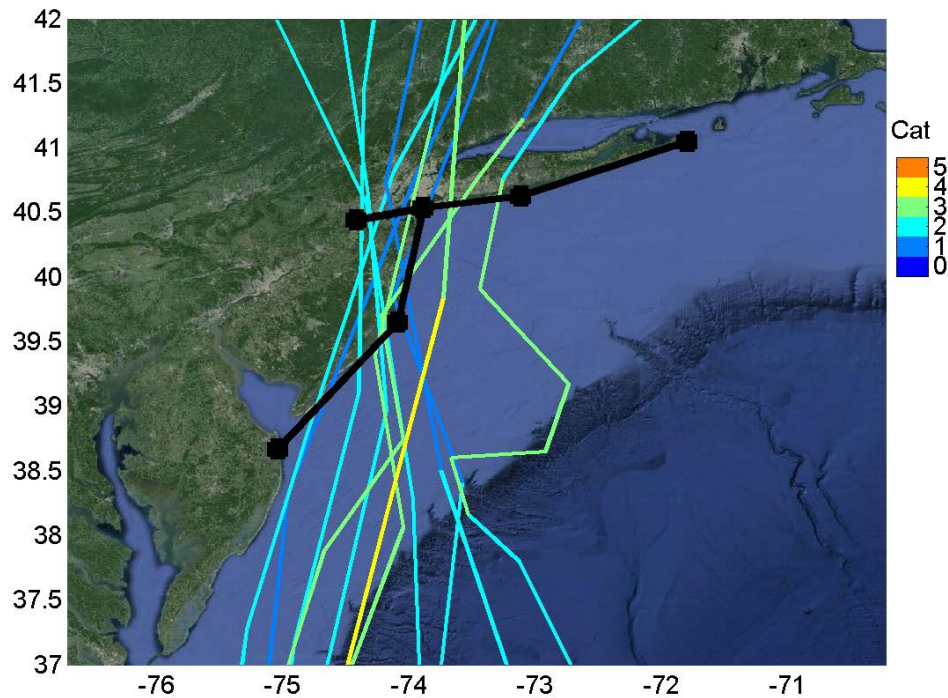


**Figure 2:** Select modeled synthetic tropical cyclone tracks colored by Saffir-Simpson category, on a map that includes the landfall gates (black lines; Orton et al., 2016). The storms that are shown lead to storm tides close to the 100-year event (2.5 - 2.9m) at The Battery (NYC) and occur at a rate higher than 0.0001 per year.

Distributions of occurrence rates for a range of water levels are constructed from model results at each model grid cell, separately for TCs, ETCs, and WETCs. These are used to compute curves showing the probability of a flood exceeding a given water level, also known as a flood exceedance curve. The probabilities for each type of storm are merged to form flood exceedance curves for any storm type. Lastly, for presentation, these data are plotted in terms of return period, which is the inverse of probability ( $1/P$ ). These computations are repeated for all grid cells within the model domain.

This joint statistical-dynamical framework for assessing the flooding hazard from storm surges with a hydrodynamic model, using a combination of historical data and synthetic hurricanes, is similar to that used for the FEMA Region II (NY/NJ) flood zone mapping effort (FEMA, 2014). However, the FEMA study

used a simplified 2D storm surge model, and included no freshwater flow from rivers. We improve upon their method by including freshwater inputs to the Hudson and using sECOM, a more detailed hydrodynamic model that has been used and validated for this region for over ten years (<http://stevens.edu/NYHOPS>), described below.

## Modeling

This study uses computer modeling instead of historical water levels for two primary reasons: (1) to estimate the water level over an entire region, not just at tide gauges, thus overcoming a limitation of tide-gauge based assessments and (2) to enable the study to account for realistic storm events and tide/storm combinations that have not occurred in the limited historical record. Synthetic events allow improved estimation of low-probability events such as the 100-year (1% annual chance) or 1000-year (0.1% annual chance) flood, provided the model is well validated against historical data.

The Stevens ECOM (sECOM) three-dimensional hydrodynamic model (Blumberg et al., 1999; Georgas & Blumberg, 2009) has been providing highly accurate storm surge forecasts on its NYHOPS grid (<http://stevens.edu/NYHOPS>) for over a decade, with mean water level errors of 0.10 m since 2007 (Georgas & Blumberg, 2009), 0.15 m for Tropical Storm Irene (Orton et al., 2012), and 0.17 m for Hurricane Sandy (Georgas et al., 2014). The NYHOPS grid includes the mid-Atlantic and northeastern U.S. coastline from Maryland to Rhode Island. For flood hazard assessment studies, the grid is nested inside a NW Atlantic model grid that captures the large-scale influence of winds from Nova Scotia to Cape Hatteras and out to approximately 2000 km distance offshore. Details of the ocean modeling, including drag coefficient parameterization, wave model coupling, and tide forcing, are all summarized in Orton et al. (2016).

TC streamflow hydrographs are modeled using a statistical Bayesian approach (Orton et al., 2018) to create streamflows for five tributaries spaced along the Hudson from north to south, and across it east to west. The chosen tributaries are the Upper Hudson (above lock 1; 11966 km<sup>2</sup>), Mohawk (8837 km<sup>2</sup>), Wappinger (469 km<sup>2</sup>), Rondout (2849 km<sup>2</sup>), and Croton (935 km<sup>2</sup>). The 10th, 50th, and 90th-percentile streamflow hydrographs are modeled for each TC, totaling nearly 2000 TC events. Our statistical TC streamflow model builds hydrographs in three pieces: (1) peak discharge (Bayesian Simultaneous Quantile Regression with TC attributes); (2) timing of the peak (multivariate normal distribution); and (3) hydrograph shape (KNN) (Orton et al., 2018).

For ETCs and WETCs, we use available historical streamflow data along the Hudson and a number of tributaries, including the Mohawk, Fort Edward, Hackensack, Passaic, Saddle, Raritan, Manalapan, Esopus, Rondout, Wallkill, Wappinger, Rahway, Croton, and Hoosic Rivers. Where only daily data are available (typically prior to 1990), the USGS peak flow estimates for major flood events are inserted into the time series on the day of the peak, to avoid underestimating peak flows during the storms. For all three storm types, ungaged or unmodeled small-to-medium tributaries (the remainder of a total of 52 Hudson River and New York Harbor region freshwater inputs to the model) are estimated using the standard NYHOPS system of estimating streamflows based on nearest similar-sized watersheds and scaled by watershed area .

Storm-driven increases to streamflow into Long Island Sound are neglected, as they have a negligible influence on the peak storm tide at those locations. Completely neglecting streamflows led to a 1% reduction in the peak storm tide at Kings Point for Hurricane Irene, in spite of its extreme rainfall (Orton et al. 2012).

To quantify error, we compare modeled water levels for 83 historical events with observations. Plots of the validation are given in **Appendix 1**, and broader details and discussion are provided in Orton et al. (2018). For ETCs The Battery root-mean-square error (RMSE) is 0.19 m (30 events), whereas for Albany RMSE is 0.14 m (5 events). For TCs, The Battery RMSE is 0.32 m (12 events), whereas at Albany the RMSE is 0.54 m (5 events). The validation for the WETC water levels at Albany shows an RMSE of 0.33 (18 events). Western Long Island Sound (Kings Point) results for ETCs have an RMSE of 0.32m, and for TCs have an RMSE of 0.64 m. Accounting for uncertainty in observations and meteorological forcing, which is especially large for the most intense storms, the results show that the model is reliable and able to represent and quantify the complex hydrodynamics of the storm-induced flows.

## Sea level rise

The mapping tool presents several sea level rise scenarios as a given, from 6 inches to 72 inches, with no context or year estimates of when they might arrive. The high value of 72 inches approximately matches the high-end (90<sup>th</sup> percentile) projections of sea level rise at the year 2100 in the most recent regional New York State sea level rise projections from the ClimAID project (71 inches at Troy Dam, 75 inches at NYC; Horton et al., 2015). The ClimAID projections account for ocean thermal expansion, local changes in ocean height, ice melt from Greenland and Antarctic ice sheets, ice melt from glaciers and ice caps, gravitational, rotational, and elastic “fingerprints” of ice loss, vertical land movements, and land-water storage (Horton et al., 2015).

The expected arrival decade for each of the specific values of sea level rise is shown in **Table 1**, and is based on simple computations made using the ClimAID report’s projections. The table presents the uncertainty as the range of decades where there is an 80% chance of seeing the given sea level rise occur. For example, the sea level scenario of 12 inches is expected around the 2040s, and there is 80% confidence it will occur between the 2020s and 2070s. The ClimAID report provides 10<sup>th</sup>, 25<sup>th</sup>, 75<sup>th</sup>, and 90<sup>th</sup>-percentile projections of sea level, and here we present low-end, median and high-end scenarios, which are 10<sup>th</sup>, 50<sup>th</sup>, and 90<sup>th</sup>-percentile values. The 50<sup>th</sup> percentile was estimated from the 25<sup>th</sup> and 75<sup>th</sup> percentile values by linear interpolation. To create these decade estimates, the available ClimAID sea level projection and year data are fitted with a 2<sup>nd</sup>-order polynomial, separately for 10<sup>th</sup>-, 50<sup>th</sup>-, and 90<sup>th</sup>-percentile sea level rise scenarios; then, exact years are taken from the fitted curves. In the table, the years are rounded to the nearest decade, and cases where the scenario would be reached after 2100 are shown as “>2100”, because the ClimAID projections are not intended to be extrapolated beyond their end date of 2100.

There is a relatively small difference of 4 inches by 2100 in vertical land movements between areas to the south and north along the Hudson (NYC is slowly sinking, Albany is not, owing to post-glacial vertical land movements lasting thousands of years; e.g. Peltier, 2004). However, we are neglecting this because it is beyond the resources of this study to map and impose the spatially varying landscape change. We

use the higher sea level rise numbers for NYC to build Table 1, conveying the scenario with a slightly more rapid sea level rise.

**Table 1:** Expected years for each sea level rise scenario, based on median, low-end (10<sup>th</sup>-percentile), and high-end (90<sup>th</sup>-percentile) sea level rise projections of sea level rise over NOAA’s 1983-2001 mean sea level datum (centered on 1992).

sea level rise	low-end scenario	Median scenario	high-end scenario
Inches	Year	Year	Year
0	1992	1992	1992
6	2030s	2020s	2010s
12	2070s	2040s	2020s
18	>2100	2050s	2030s
24	>2100	2070s	2040s
30	>2100	2080s	2050s
36	>2100	2090s	2060s
48	>2100	>2100	2070s
60	>2100	>2100	2080s
72	>2100	>2100	2090s

The vertical datum are important for flood mapping. The ClimAID projections are sea level change over the 2000-2004 mean sea level for NYC, so to correct these to the NOAA datum of 1983-2001 mean sea level (with a mid-point of 1992 used in **Table 1**) we add 1.1 inches (10 years of sea level rise at the historical average rate at NYC).

### Flooding from tides with sea level rise

Tidal flooding is quantified with three-dimensional hydrodynamic simulations of tides using the NYHOPS forecasting system’s operational setup, under tide and mean streamflow forcing (no wind). Simulations cover a 35-day period beginning August 1, 2015. This approach for modeling tides to estimate tide datums with sea level rise was recently used in studies of Long Island Sound and Jamaica Bay. It gives accurate estimates of tidal datums when compared to multiple years of local tide gauge observations (Fischbach et al., in preparation; Kemp et al., 2017; Smith et al., in preparation). Model results are subjected to tidal harmonic analysis (Pawlowicz et al., 2002), to fully represent 19-year tidal variability and all the periodicities therein. Resulting Mean Higher-High Water (MHHW; the average daily high tide level) estimates are bias-corrected to observation-based MHHW estimates at 11 stations along the Hudson from Westchester County northward (Georgas et al., 2013) and 2 stations in Western Long Island Sound (NOAA, 2017). The biases for the zero sea level rise case are then applied to all results for

the 10 sea level rise scenarios. A more detailed description of methods, bias correction and model-observation comparisons is included in **Appendix 1**.

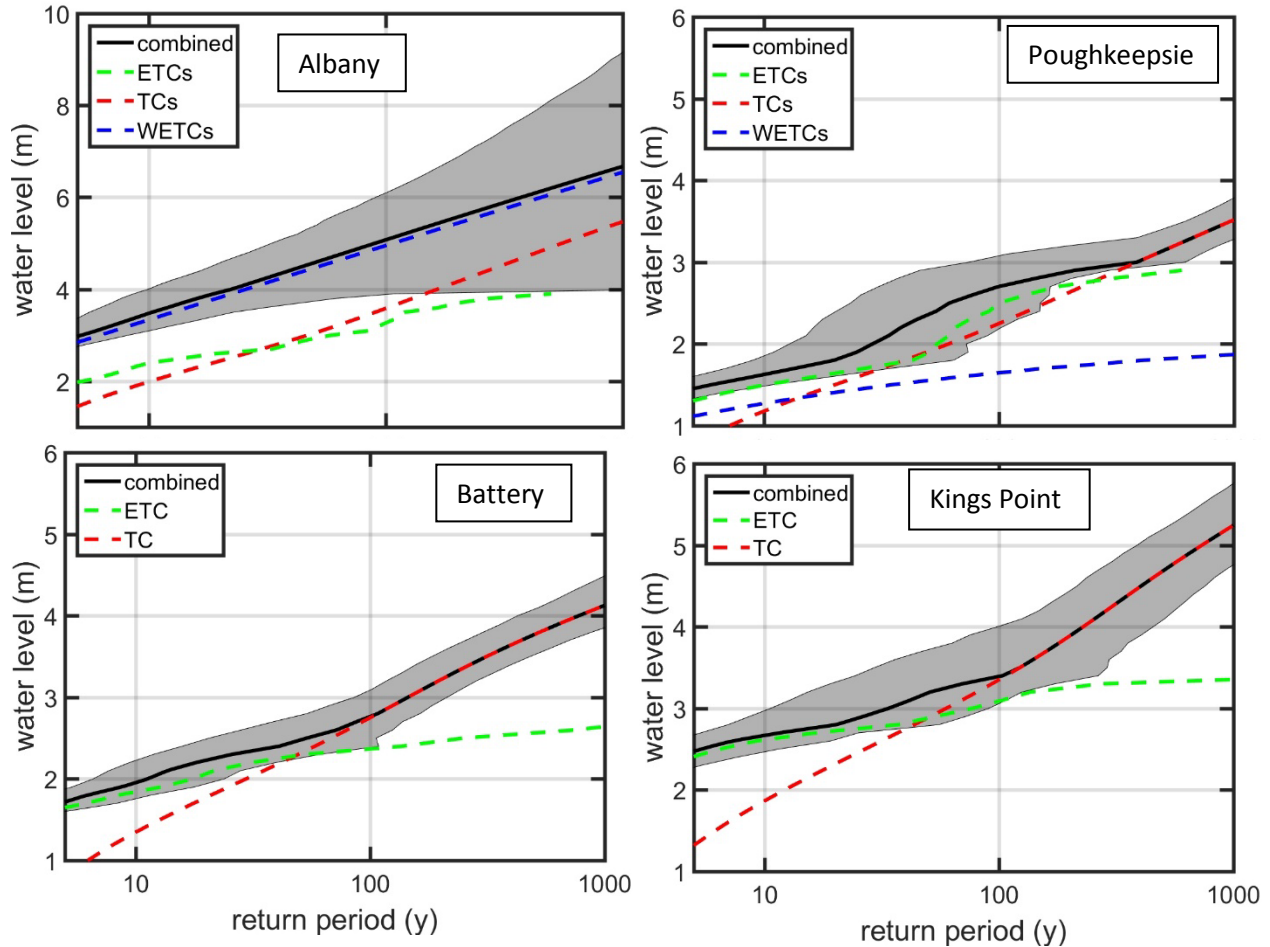


**Figure 4:** Flood return period curves – black lines show the combined flood hazard assessment, merging exceedance probabilities from TCs, ETCs, and WETCs, and grey areas show 95% confidence intervals (Battery and Kings Point only show TCs and ETCs because WETCs had a negligible impact). Note different y-axis scales.

## Flood Scenarios: Results

### Storm tides with sea level rise

Each type of storm is separately modeled and flood return periods statistically evaluated, including 95% confidence intervals. Monte Carlo methods are used to assess the propagation of model error through the analysis, and bootstrap methods are used for re-sampling storms to incorporate the uncertainty of

the limited ETC and WETC storm sets (Orton et al., 2016). Detailed results for model validations, flood levels and uncertainties from each type of storm are given in Orton et al. (2018).

Flood exceedance probabilities for each type of storm are merged to create the combined flood exceedance curves, representing the return period for any type of flooding along the Hudson. Similar data are available for all grid cells within the model domain. The curves show that Albany results are dominated by WETCs (**Figure 4**). Poughkeepsie results show a flood hazard that is a mixture of all three storm types. NYC results at both The Battery and Kings Point show a dominance of TCs for the 100-year flood, and ETCs for the 10-year flood.

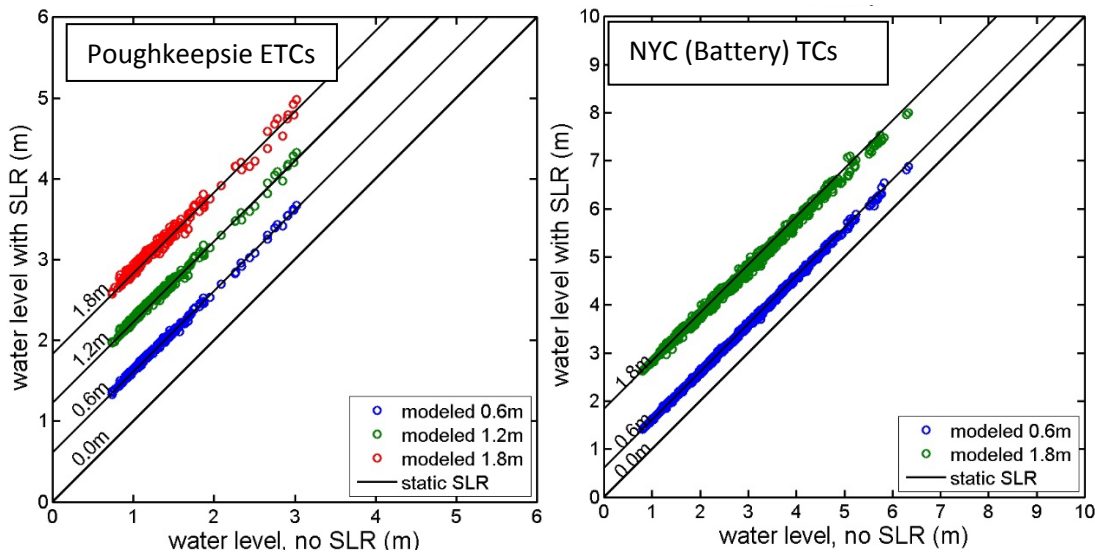


**Figure 5:** Change in water level for various amounts of sea level rise for (left) Poughkeepsie for ETCs, and (right) for NYC (Battery) for TCs. In both cases, model results are very close to the static assumption (simple superposition of water level and sea level rise), and this is also the case for TCs at Poughkeepsie and ETCs at NYC (Orton et al., 2018).

However, the results at Albany show large deviations from a simple static sea level rise approach (**Figure 6**). Water levels for WETCs are below the static assumption and water levels for ETCs are above the static assumption. The WETC result occurs because a deeper river has less of a frictional effect on a flood, which favors the escape toward the ocean of the river floodwater. That is, the sea level rise may cause higher water, but it also ameliorates the floodwater pulse, and ultimately, the total is less than the sum of the two. The ETC result likely occurs for a similar reason, though flipped around – ocean tides (and surge) are propagating over 200 km up the Hudson through deepened water due to sea level rise, and therefore have less frictional damping and are larger once they reach Albany (Orton et al., 2018).

## Tides with sea level rise

Results for the MHHW tidal datum demonstrate how sea level rise can increase tidal water levels, and again there are cases with deviations from static superposition. **Figure 7** shows the “nonlinear sea level rise”, which is the modeled flood level above simple superposition of tidal MHHW and sea level rise.

The resulting nonlinear sea level rise is generally zero or positive, indicating that floods are higher than superposition would predict – as much as 20 cm at some locations (~11% of the sea level rise). A similar pattern is seen across all sea level rise scenarios, and is exemplified by the cases shown in Figure 4 (0.91 and 1.83 m). These show nonlinear sea level rise contributions of about +2% at the seaward end of the Hudson and about +10% in the upper half of the tidal Hudson.

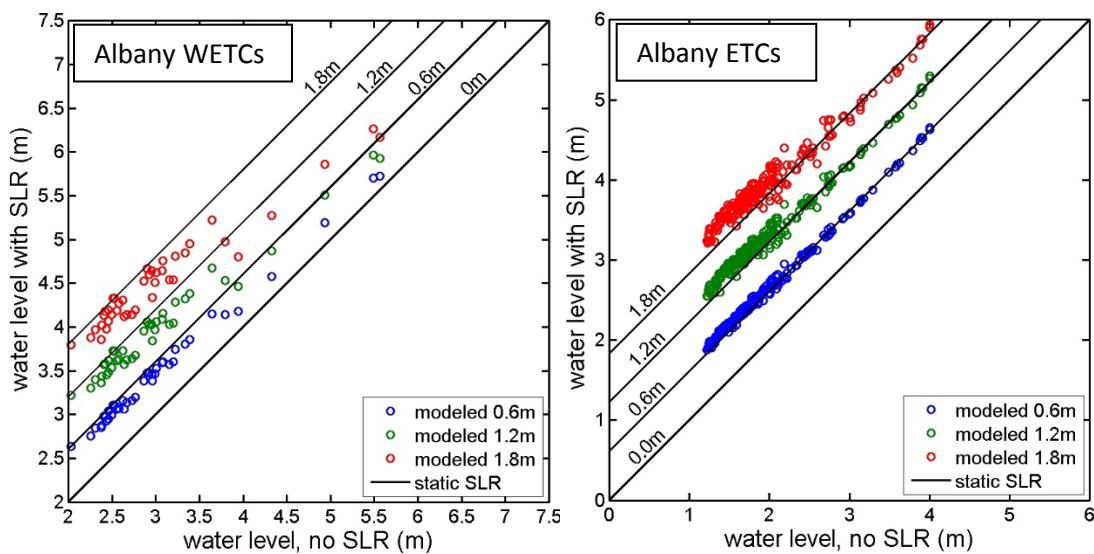


**Figure 6:** Change in water level with various amounts of sea level rise at Albany, for (left) WETCs and (right) ETCs. For WETCs, water levels are lower than the static sea level rise assumption. For ETCs, water levels are higher than that static assumption (Orton et al., 2018).

These results are unsurprising, given the similar finding for ETCs in the existing data report’s figure 6 right-side panel. Under cases with low or mean streamflows, sea level rise deepens the water column, enabling decreased tidal frictional dissipation or enhanced reflection at the head-of-tide (Troy, NY), and as a result the modeled combination of storm tide (or simply tide) plus sea level rise is higher than their sum.

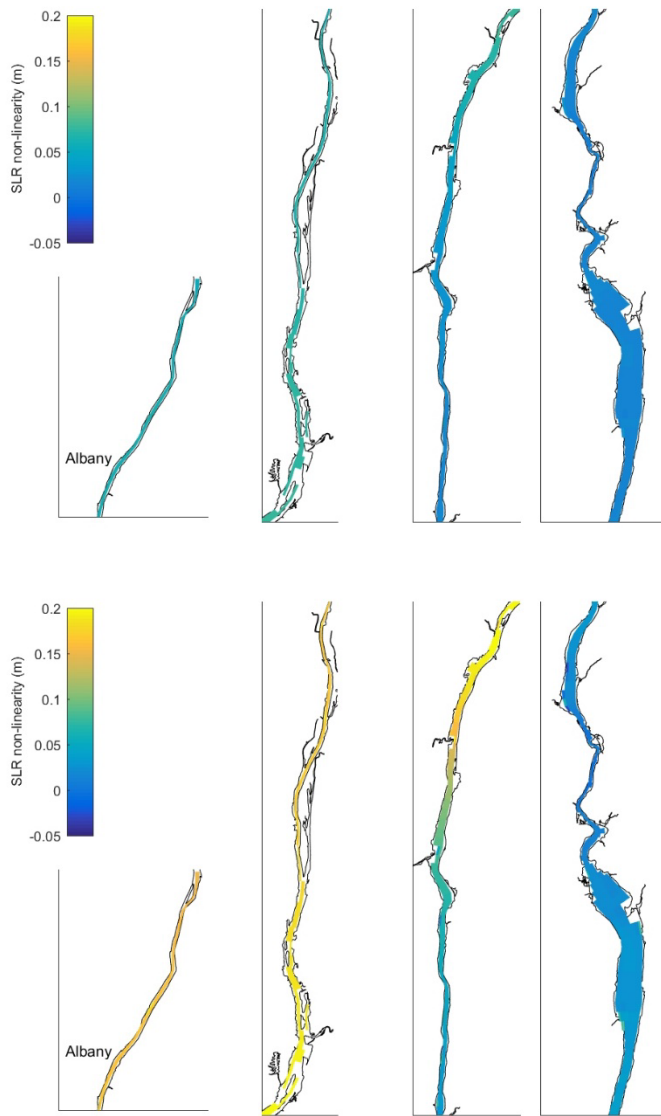


**Figure 7:** “Nonlinear sea level rise” – the modeled flood level above simple superposition of tidal MHHW plus sea level rise (above static sea level rise). The top panel shows the result for sea level rise of 0.91 m, and the bottom panel for sea level rise of 1.83 m. Values are generally zero or positive, indicating that floods are higher than superposition would predict – as much as 20 cm at some locations (~11% of the sea level rise).

## Mapping

LiDAR data from NYSDEC is used at 1 meter horizontal pixel resolution. We consider the maximum range of still water elevation (SWEs) estimates across the full set of modelled flood scenarios in order to determine the maximum depth of flooding, which is approximately 12 vertical meters. We next subset the LiDAR data in order to remove any elevation pixels with a value greater than 12 meters. This forms the maximum possible extent of the flood plain used for bathtub modeling.

- Density of estimates
- Trend of estimates

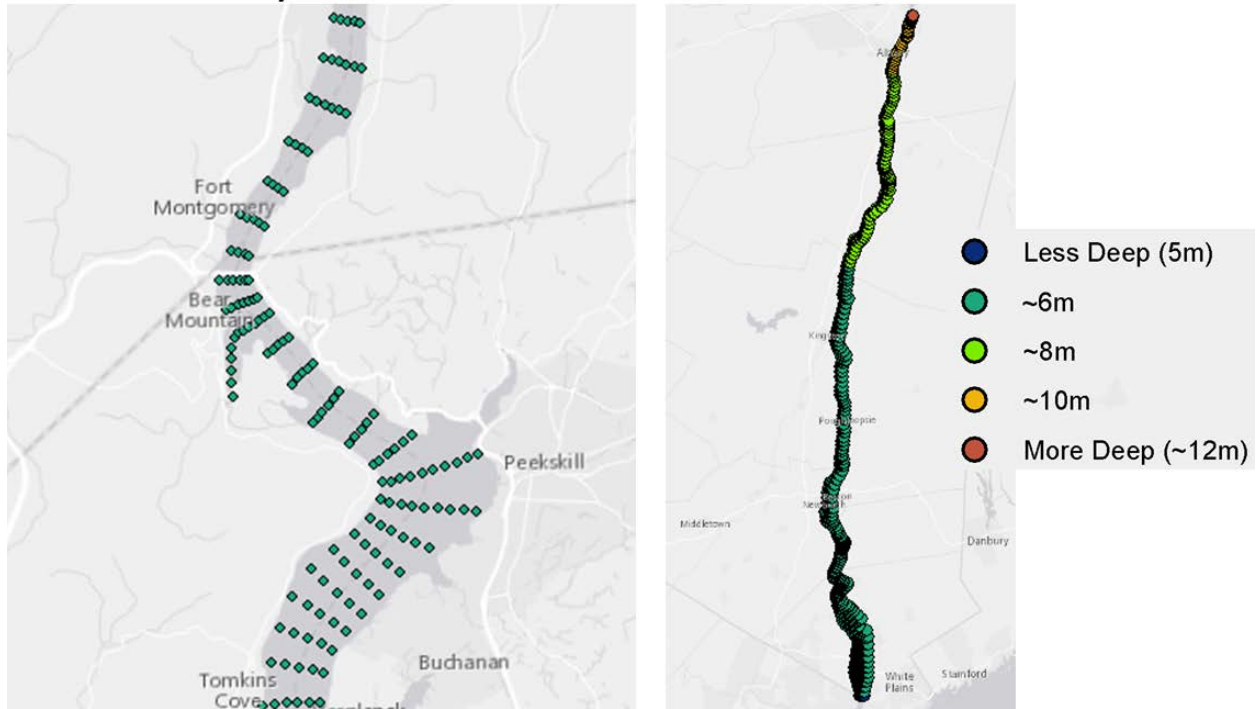


**Figure 7:** Maps of the density and depth of estimate points from the Stevens NYHOPS domain.

The bathtub method is implemented by first interpolating the SWEs estimate points depicted in **Figure 7** onto the <12 meter maximum flood plain extent. A radial basis function is applied to the SWE estimate points in order to create interpolated surfaces. Finally, the interpolated scenarios are subtracted from the LiDAR ground elevation in order to derive flood depths.

The bathtub process results in the selection of some low-lying areas that are not surficially connected to the river channel according to the LiDAR data. However, these areas may still be at risk of flooding if they are connected below ground naturally or through man-made infrastructure such as culverts. Rather than remove these areas from the final flood scenario data, they are recoded as “Possible Flooding – Disconnected.” Additional research is needed to determine if there is, in fact, hydrologic connectivity in these areas.

## Social Vulnerability

The social vulnerability index is a multidimensional measure that identifies block groups and municipalities along the Hudson River with a high likelihood of sustaining losses from, or an insufficient capacity for resilience to Hudson River flood hazards.

Constructing the indicator was a multi-step process. First, we looked at past literature to identify the diverse dimensions of vulnerability relevant to the study area. Second, we identified quantifiable measures for each of the sub-dimensions of vulnerability. As seen in **Appendix 2**, the number of variables used to measure each vulnerability dimension varies, mainly because of data availability. A more detailed discussion regarding the variable selection is presented below. Third, we created the index using the following processes: cleaning the data; transforming the data when necessary to ensure data completeness; normalizing data; reducing the data to a select few complex dimensions of vulnerability using principal component analysis; and calculating the social vulnerability index using two different aggregation methods.

## Theoretical framework

The theoretical framework of our index is based on the dimensions of vulnerability that are most commonly found in the literature: social characteristics, economic status, isolation, and health (Cutter et al., 2003). **Appendix 2** presents a description of the framework including the dimensions and sub-dimensions of vulnerability, along with the variables used for measuring each dimension.

### Social Characteristics

We focused on social characteristics of vulnerability in which the ascribed social status is assigned at birth or assumed involuntarily later in life, including race/ethnicity, age, and gender. Language can also affect access to necessary information pre- and post-disaster, as well as access to post-disaster funding. Cultural barriers can influence people's decisions during a disaster event and may also be a vulnerability factor. Underrepresented minorities are historically more likely to experience losses from disaster events. Looking at vulnerability based on age, the elderly population may experience obstacles in both mobility and access to information. Young people have a different type of vulnerability due to dependency on caregivers during the time of disaster. Families with young children, particularly female-headed households, are likely to be more vulnerable post-disaster when parents cannot find available childcare.

### Economic status

Differences in economic status expressed in variables like poverty level, occupation, housing, and education have a large impact on preparedness and response to a disaster. People living in poverty before a disaster lack the necessary resources for recovery. Among low-income households, at greater risk are populations with vulnerable social status (children, the elderly, underrepresented minorities, and women). Economic status is influenced by education, as low education achievement can lead to low-paying jobs and fewer resources for recovery post-disaster. The type of housing is also important: renters may not be able to find shelter post-disaster, according to Cutter et al. "People that rent do so because they are either transient or do not have the financial resources for home ownership. They often lack access to information about financial aid during recovery. In the most extreme cases, renters lack

sufficient shelter options when lodging becomes uninhabitable or too costly to afford". Additionally, the number of people impacted by a disaster is generally higher for multi-family buildings.

### Isolation

The likelihood of loss of transportation infrastructure is high during disaster events, thus the level of isolation will influence post-disaster recovery. Access to public or personal transportation, distance to work, and access to phone communication greatly influence the extent of loss during and post disaster.

### Health

Access to health care facilities is of most importance during disaster events, and has great impacts on loss or capacity of recovery after the event.

### Variable selection

After identifying vulnerability dimensions, we collected variables that measure each of these thematic categories. In accordance with previous similar analyses, our main data source of proxy measures for the vulnerability dimensions stated above was the American Community Survey (ACS) conducted by the US Census Bureau. For this analysis we used the 2007-2011 ACS results, which are available in tabular and spatial format (i.e. polygon). In addition, a few isolation and health measures were processed by CIESIN based on infrastructure data available from ESRI.

At different stages of the analysis, our dataset included varying numbers of input variables. The 31 variables that were finally included were the best at measuring the dimensions and sub-dimensions of vulnerability listed in **Appendix 2**.

### Indicator construction

The data includes only New York State counties along the lower Hudson River north of New York City: Albany, Columbia, Dutchess, Greene, Orange, Putnam, Rensselaer, Rockland, Ulster, and Westchester.

The analysis was conducted at both the block group and municipality level in order to make comparisons based on both sets of administrative units.

### Data cleaning

First, the raw tabular datasets were cleaned and prepared for use. The spatial database included 2,116 block groups, from which we omitted 4 block groups with no population, 10 block groups with no households and 1 block group with no per capita income. The same input data could then be divided into 162 municipalities across the 10 counties.

### Data transformation and normalization

The raw data values for the 2,101 remaining block groups and 162 municipalities were transformed by dividing by the total population of interest in order to make the data comparable across counties. In addition, per capita income was inverted to ensure that low values correspond to high incomes which represent low vulnerability, and high values correspond to low incomes which represent high vulnerability. The calculation used for each of the variables is presented in the last column of **Appendix 2**.

Some of the block groups may have zero population of a given variable of interest, which could potentially lead to missing values. For example, the “percent of the population over 65 living alone” variable is calculated by dividing the population over 65 living alone by the total population over 65. In our dataset, there were 19 block groups with no population over 65 years old. These block groups were considered to have low vulnerability for this variable, therefore the 19 missing values were recoded as zero which is the lowest vulnerability value. This type of transformation was not necessary at the municipal level.

Finally, we normalized the variables by centering (extracting the mean) and scaling (dividing by standard deviation). As a result, the variance of each of the variables included in the analysis is one, and the total variance in the dataset is 31 (equal to the total number of variables in the dataset).

### Data reduction

We used principal component analysis (PCA) to reduce the number of variables to a set of uncorrelated latent components that keep most of the variance of the original variables. At the block group level, the first five components resulting from the PCA algorithm explain 51.44% of the variation in the 31-variable dataset, while at the municipal level the variance explained by the same number of components is 62.99%. There are several methods used in the literature with regard to the PCA component selection: Keiser criterion, Horn parallel analysis, the percentage of variance explained, and expert choice. We used the percentage of variation explained to select the first five components (see **Appendix 3**, column 3 for block group level, and **Appendix 4**, column 3 for municipal level).

We named remaining components according to the dominant variables within each component. The dominant variables were determined from variable loadings, which are equivalent to correlation coefficients (see **Appendix 3**, last column for block group level, and **Appendix 4**, last column for municipal level). Values closer to 1 represent high vulnerability, while those closer to -1 represent low vulnerability. In some cases, the high-vulnerability components were loading with negative values (see dimensions 1 and 5 for municipal level); therefore, we inverted the values so that high values represent high vulnerability. In other cases we noticed a strong relationship on both negative and positive sign, and we calculated the absolute value of that variable. For example, median age and the percentage of population over 65 living alone load positively on Housing and Age dimension (block group level), while population under 5 loads negatively.

### Output vulnerability dimensions

Each of the five dimensions of social vulnerability was constructed based on a combination of vulnerability aspects present in the input data. The first output dimension of vulnerability, deprivation, has elements that correspond to housing, poverty, and isolation, and explains 28% of the original variance at the block group level (31.55% for the municipal level).

Isolation is the second social vulnerability dimension resulting from PCA, and explains 7.56% of the variance at the block group level, with public transportation and long work commute as the most significant variables. At the municipal level, the second dimension, “Isolation and thnicity” is more

complex, and explains ~15% of variance. Along with isolation elements, it is also correlated with ethnicity and housing variables.

The third dimension of social vulnerability is Housing and Age, which captures youth and elderly vulnerability and housing structure. It explains 6.35% of the variance at the block group level (6.10% at the municipal level).

The remaining two dimensions represent different combinations of variables for block groups and municipalities and explain variance less than the first three. For block groups, the Ethnicity and Occupation dimension includes variables on underrepresented minorities, employment, and isolation, and the Dependency dimension is a mix of age, race, education, housing, gender, and unemployment. At the municipal level, the Dependency dimension appears with a similar mix, and is higher in importance (4th component). Remoteness accounts for isolation and health access.

### **Aggregation**

Most previous social vulnerability studies aggregated the principal components using an additive method (Tate, 2012). The method is simply summing up all the principal components. For the second aggregation method, we used the eigenvalues (variance) of each component as a weight.

#### ***Social Vulnerability equation – block group level:***

Additive method:

$$\text{SOVI} = \text{PC1} + \text{PC2} + \text{abs}(\text{PC3}) + \text{PC4} + \text{abs}(\text{PC5})$$

Weighted method:

$$\text{SOVI}_w = \text{PC1} * (\text{PC1 eigenvalue}) + \text{PC2} * (\text{PC2 eigenvalue}) + \text{abs}(\text{PC3}) * (\text{PC3 eigenvalue}) + \text{PC4} * (\text{PC4 eigenvalue}) + \text{abs}(\text{PC5}) * (\text{PC5 eigenvalue})$$

#### ***Social Vulnerability equation – municipal level:***

Additive method:

$$\text{SOVI} = (-1) * \text{PC1} + \text{PC2} + \text{PC3} + \text{abs}(\text{PC4}) + (-1) * \text{PC5}$$

Weighted method:

$$\text{SOVI}_w = (-1) * \text{PC1} * (\text{PC 1 eigenvalue}) + \text{PC2} * \text{PC2 eigenvalue} + \text{PC3} * (\text{PC 3 eigenvalue}) + \text{abs}(\text{PC4}) * (\text{PC 4 eigenvalue}) + (-1) * \text{PC5} * (\text{PC5 eigenvalue})$$

abs() represents absolute value.

The subscript w indicates the weighted SOVI score.

A set of impact estimates accompany each of the flood scenarios presented in the Mapping Tool. The impacts are divided into three sets of results: Critical Infrastructure (including estimated losses), Climate Smart Communities, and Social Vulnerability.

## Impact Estimates

A set of impact estimates accompany each of the flood scenarios presented in the Mapping Tool. The impacts are divided into three sets of results: Critical Infrastructure (including estimated losses), Natural Resilience, and Social Vulnerability.

Version 2.2 of the FEMA-developed HAZUS-MH Flood model was generalized for automation of 90 divergent Sea Level Rise and Storm Tide scenarios using user-defined data for building stock and flood depths. Analysis was completed at the building footprint level and then aggregated to block groups, municipalities, and counties. Tax parcel data was converted into HAZUS-MH building occupancy classes and assigned to building footprints. Where tax parcel data on required attributes was not available, block level data from HAZUS-MH was used to infill building footprint attributes. Depth Damage Functions were then applied to each building before aggregation. The resulting output statistics include the number of damaged buildings, as well as the estimated financial loss associated with the flood event.

## Critical Infrastructure

Our geographic database of critical infrastructure consists of a variety of structures at risk from flood events including:

airports, boat launches, bridges, bus routes, bus stations, dams, DEC roads trails, EIA power plants, emergency operations centers, EMS, fire stations, heliports, hospitals, large culverts, linear hydrography, nursing homes, places of worship, police stations, power transmission lines, prisons, public libraries, railroad junctions, railroad passenger stations, railroads, schools, SPDES wastewater sites, water wells, and water withdrawal locations.

Impacts to critical infrastructure were calculated using an overlay analysis of each of the flood scenario surfaces. For point data, a facility was considered impacted if and when it was intersected by any amount of flooding (i.e., in the flood zone) for a particular scenario. For line data, the linear section of the feature intersected by flooding was calculated and is presented in the mapping tool and the statistical download files.

## Natural Resilience Features

Natural areas like forests, wetlands, and floodplains are vital assets to consider in assessing vulnerability and planning for resilience. In contrast to impervious surfaces in developed areas, these natural features retain, slow, filter, and infiltrate water to the soil, reducing erosion and flood impacts. Conserving and managing natural assets is thus an important resilience strategy.

Descriptive statistics of several spatial data sets for natural features are summarized at the municipal level and in the area estimated to be impacted by the selected flood scenario. Impervious surface area is also described.

Large, intact forests, wetlands, and floodplains that provide connectivity between natural areas are most likely to maintain natural processes contributing to resilience and will facilitate the migration of plants and animals as climate changes. Used together with the ecology and infrastructure layers, these results allow you to analyze spatial patterns and to locate areas of particular vulnerability as well as natural areas of greatest importance to slow and store water during a flood.

The variables summarized for each scenario and location include:

- Total land area(acres)
- Total forest (acres)
- Percent forested (%)
- Total NWI wetlands (acres)
- Total tidal wetlands (acres)
- Total impervious surface area (acres)
- Percent impervious (%)
- Inundated land area in this scenario (acres)
- Inundated forest(acres)
- Inundated NWI wetlands (acres)
- Inundated impervious surface area (acres)

## **Social Vulnerability**

The Social Vulnerability Index (SoVI) was developed to map populations at risk from predicted flood events and is described fully in the Social Vulnerability section of this report.

The impact estimates for this thematic area include the decile rank of the impacted block groups in each municipality for each component of the index and the average rank of all of the blocks in each municipality. A high ranking indicates high vulnerability, while a low ranking indicates low vulnerability.

Used together with the social vulnerability layers, the results allow for a comparison of vulnerabilities both within a municipality and against other municipalities.

## **Climate Smart Communities Flood Adaptation Guidance**

The variables highlighted in this section appear in the map application and are emphasized here on the basis of recommended flood adaptation strategies in the New York State Department of Environmental Conservation (NYSDEC) Climate Smart Communities Certification Manual (<http://www.dec.ny.gov/energy/50845.html>). The Certification Manual outlines steps municipalities can take to reduce flood risk and identify and protect important natural features contributing to community resilience. Refer directly to “Pledge Element 7” of the Climate Smart Communities Certification Manual for more information.

## Dams

Old or improperly maintained dams can present a flooding hazard to the surrounding communities in the event of dam failure or intense precipitation.

**Adaptation Strategy** - Remove unnecessary and hazardous dams.

## Bridges and Culverts

Improperly sized culverts and bridges can contribute to localized flooding near stream-road crossings, and present a hazard to the community if they are routinely overtopped or blowout.

**Adaptation Strategy** - Right-size bridges and culverts to provide suitable capacity in flood events and ensure proper installation to allow fish passage.

## Impervious Surface

Impervious surfaces such as roofs, roads, parking lots, and other paved areas dramatically increase and change the timing of stormwater runoff, often exacerbating local flooding.

**Adaptation Strategy** – Concentrate new development in existing centers, reduce impervious surfaces, and use green infrastructure practices to reduce stormwater runoff.

## Forest Cover

Forests are very effective at limiting stormwater runoff by intercepting precipitation and promoting infiltration to the soil. In addition, riparian forests dissipate flood energy.

Large, intact, connected forests contribute to ecosystem resilience and facilitate migration of plants and animals.

**Adaptation Strategy** - Avoid further fragmentation and loss of function or integrity of forests, restore forest along streams and in floodplains, and conserve or restore broad linkages between forest patches to facilitate species migration.

## Wetlands

Both tidal and non-tidal wetlands can absorb and hold large quantities of water, filtering and slowly releasing it, reducing flood impacts and improving water quality. Tidal wetlands also help to buffer impacts from storm surge and provide critical habitat for estuary fish and wildlife species.

**Adaptation Strategy** – Avoid further wetland loss and conserve wetland buffers to protect wetland function and integrity. Conserve or restore linkages between wetlands and potential future tidal zones to facilitate species movement and tidal wetland migration.

## Floodplains

By slowing and storing floodwaters, floodplains reduce downstream flood damage and serve as a safety zone between human settlement and the damaging impacts of floods.

**Adaptation Strategy** – Conserve and revegetate floodplains and other streamside (riparian) buffers. It is also critical to ensure that streams are connected to their floodplains, so that floodwaters have a place to go. Remove berms, levees or other built barriers that block floodwaters from accessing floodplains to allow those areas to once again collect, store and slow water movement during and after storm events.

### **Important Areas for Rare Plants, Rare Animals, and Significant Natural Communities**

Many natural systems and the benefits they provide people are at risk due to climate change and other stressors. Large, natural areas with diverse physical conditions and little fragmentation by roads or development are most likely to maintain diverse ecosystems and ecological processes contributing to resiliency. The New York Natural Heritage Program has identified important areas for sustaining known populations of rare plants, rare animals, and significant natural communities based on habitat requirements and areas critical to maintaining those habitats.

**Adaptation Strategy** - Conserve natural areas for species migration and ecosystem resilience

### **Acknowledgements**

We would like to acknowledge the vision and leadership of Mark G. Becker (1961-2014), who was the original Principal Investigator for this research, and without whom we would have never realized this work.

This research was supported by New York State Energy Research and Development Authority (NYSERDA; Blumberg, PI), the NASA Centers call for support of the National Climate Assessment (Hall, PI), the NOAA-RISA project "Consortium for Climate Risk in the Urban Northeast" (Rosenzweig, PI) and a NASA Interdisciplinary Research in Earth Science project (Kushnir, PI). Modeling was made possible by a grant of computer time from the City University of New York High Performance Computing Center under NSF Grants CNS-0855217, CNS-0958379 and ACI-1126113.

## References

- Blumberg, A. F., Khan, L. A., & St John, J. (1999). Three-dimensional hydrodynamic model of New York Harbor region. *Journal of Hydraulic Engineering*, 125(8), 799-816.
- Cutter, S. L., Boruff, B. J., & Shirley, W. L. (2003). Social vulnerability to environmental hazards. *Social science quarterly*, 84(2), 242-261.
- Department of Commerce. (2011). *New York State Department of Environmental Conservation (NYSDEC) Lidar: Coastal New York (Long Island and along the Hudson River)*, Department of Commerce (DOC), National Oceanic and Atmospheric Administration (NOAA), National Ocean Service (NOS), Office for Coastal Management (OCM), accessed at <http://coast.noaa.gov/dataviewer/index.html?action=advsearch&qType=in&qFld=ID&qVal=1408> on July 10, 2015.
- FEMA. (2014). Region II Coastal Storm Surge Study: Overview. In M. Risk Assessment, and Planning Partners (Ed.), (pp. 15). Washington, DC: Federal Emergency Management Agency.
- Fischbach, J., Smith, H., Fisher, K., Orton, P., Sanderson, E., Marsooli, R., . . . others. (in preparation). Integrated Analysis and Planning to Reduce Coastal Risk, Improve Water Quality, and Restore Ecosystems: Jamaica Bay, New York. Final project report.
- Georgas, N. (2010). *Establishing confidence in marine forecast systems: The design of a high fidelity marine forecast model for the NY/NJ harbor estuary and its adjoining coastal waters*, PhD dissertation, Department of Civil, Environmental and Ocean Engineering. Stevens Institute of Technology, Hoboken, New Jersey.
- Georgas, N., & Blumberg, A. F. (2009, 4-6 November). *Establishing Confidence in Marine Forecast Systems: The Design and Skill Assessment of the New York Harbor Observation and Prediction System, Version 3 (NYHOPS v3)*. Paper presented at the Eleventh International Conference in Estuarine and Coastal Modeling (ECM11), Seattle, Washington, USA.
- Georgas, N., Orton, P., Blumberg, A., Cohen, L., Zarrilli, D., & Yin, L. (2014). The impact of tidal phase on Hurricane Sandy's flooding around New York City and Long Island Sound. *Journal of Extreme Events*. doi: 10.1142/S2345737614500067
- Georgas, N., Wen, B., & Zhao, Y. (2013). Calculation of vertical tidal datums for the tidal Hudson River north of Yonkers, New York (pp. 25). Technical Report 2926, Stevens Institute of Technology.
- Hall, T., & Yonekura, E. (2013). North American tropical cyclone landfall and SST: A statistical model study. *Journal of Climate*, 26(21), 8422-8439.

- Horton, R., Bader, D., Rosenzweig, C., DeGaetano, A., & Solecki, W. (2015). *Climate Change in New York State: Updating the 2011 ClimAID Climate Risk Information, Supplement to NYSEDA Report 11-18 (Responding to Climate Change in New York State)*. Albany, NY.
- Kemp, A. C., Hill, T. D., Vane, C. H., Cahill, N., Orton, P. M., Talke, S. A., . . . Hartig, E. K. (2017). Relative sea-level trends in New York City during the past 1500 years. *The Holocene*, 0959683616683263.
- NOAA. (2017). Tides and Currents, National Oceanographic and Atmospheric Administration, <https://tidesandcurrents.noaa.gov/>, accessed 2017 November 1. from <https://tidesandcurrents.noaa.gov/>
- Orton, P., Georgas, N., Blumberg, A., & Pullen, J. (2012). Detailed modeling of recent severe storm tides in estuaries of the New York City region. *Journal of Geophysical Research*, 117, C09030. doi: 10.1029/2012JC008220
- Orton, P. M., Conticello, F. R., Cioffi, F., Hall, T. M., Georgas, N., Lall, U., . . . MacManus, K. (2018). Flood hazard assessment from storm tides, rain and sea level rise for a tidal river estuary. *Natural hazards*, 1-29. doi: 10.1007/s11069-018-3251-x
- Orton, P. M., Hall, T. M., Talke, S., Blumberg, A. F., Georgas, N., & Vinogradov, S. (2016). A Validated Tropical-Extratropical Flood Hazard Assessment for New York Harbor. *Journal of Geophysical Research*, 121. doi: 10.1002/2016JC011679
- Orton, P. M., & Visbeck, M. (2009). Variability of internally generated turbulence in an estuary, from 100 days of continuous observations. *Continental Shelf Research*, 29(1), 61-77.
- Pawlowicz, R., Beardsley, B., & Lentz, S. (2002). Classical tidal harmonic analysis including error estimates in MATLAB using T\_TIDE. *Computers & Geosciences*, 28(8), 929-937.
- Peltier, W. (2004). Global glacial isostasy and the surface of the ice-age Earth: the ICE-5G (VM2) model and GRACE. *Annu. Rev. Earth Planet. Sci.*, 32, 111-149.
- Smith, H., Fisher, K., Orton, P., Marsooli, R., Sanderson, E., & Roberts, H. (in preparation). untitled manuscript.
- USGS. (2014). United States Geological Survey National Water Information System (NWISWeb) online data, <https://nwis.waterdata.usgs.gov/usa/nwis>, accessed December, 2014. <http://waterdata.usgs.gov/nwis/>

## Appendix 1. Detailed Methods and Model Validations

### Storm flood modeling validations

Comparisons of historical observed and modeled temporal maximum water levels are shown for each storm type in **Figure A1**, generally showing good agreement and helping quantify model error for our uncertainty analysis. In each case, the actual streamflows and meteorological forcing methods used in the probabilistic assessment are utilized. In the case of the TCs, synthetic streamflows at the same percentile of the actual historical event for each river basin were used, and these were created using out-of-sample statistical modeling (Orton et al., 2018). A second figure shows the additional validation performed for storm modeling results at western Long Island Sound (**Figure A2**).

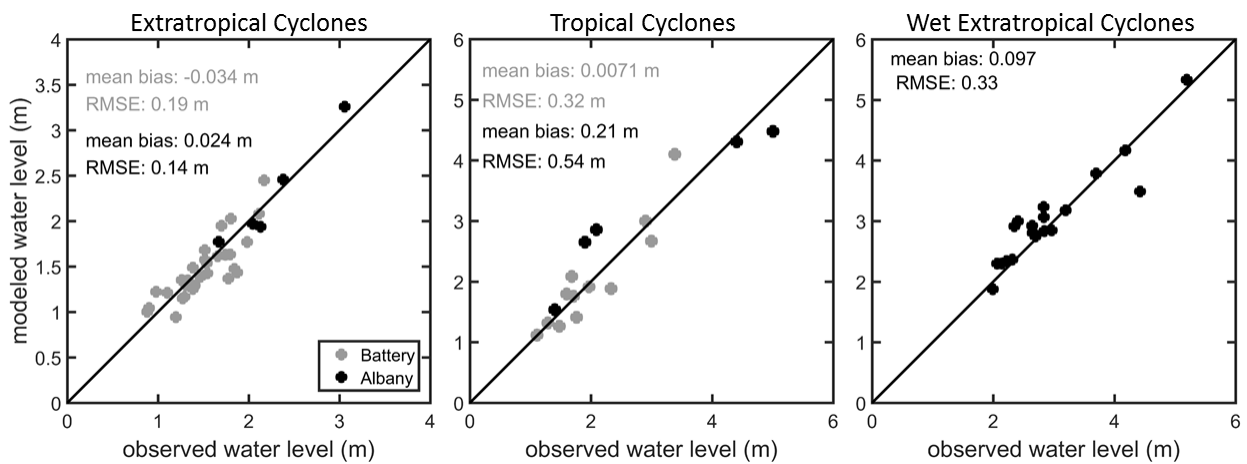


**Figure A1:** Model-observation comparisons for peak water levels for the three storm types using available data along the Hudson River (Orton et al., 2018).

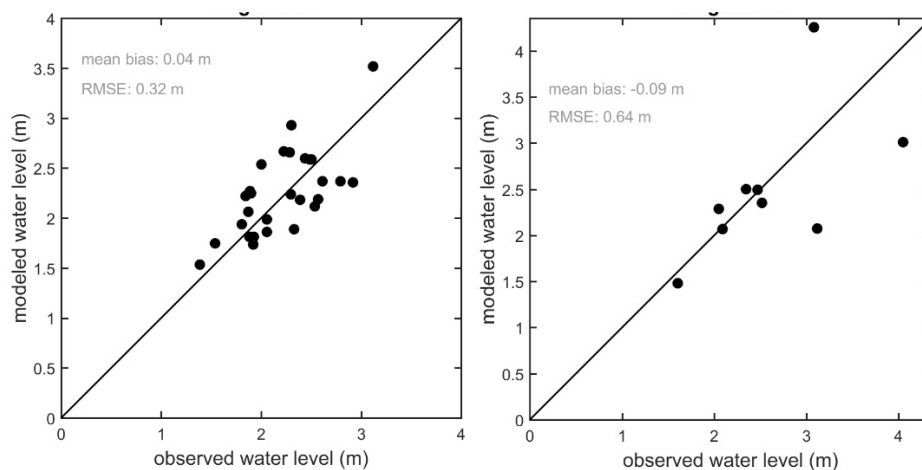


**Figure A2:** Model-observation comparisons for ETCs (left) and TCs (right) at western Long Island Sound (Kings Point and neighboring Willet's Point for older storms).

## Tidal flood assessment

Three-dimensional hydrodynamic simulations of tides were performed using the NYHOPS forecasting system's operational setup under tide and streamflow forcing (no wind), covering a 35-day period beginning August 1, 2015. This approach for modeling tides was used recently in studies of Long Island Sound and Jamaica Bay, and it gives accurate estimates of tidal datums when compared to multiple years of local tide gauge observations (Fischbach et al., in preparation; Kemp et al., 2017; Smith et al., in preparation). Model results were subjected to tidal harmonic analysis (Pawlowicz et al., 2002), to fully represent 19-year tidal variability and all the periodicities therein. Resulting Mean Higher-High Water (MHHW) estimates were bias-corrected to observation-based MHHW estimates at 11 stations along the Hudson from Westchester County northward (Georgas et al., 2013) and 2 stations in Western Long Island Sound (NOAA, 2017). The biases for the zero sea level rise case were then applied to all results for the 10 sea level rise scenarios.

The 35-day tide simulations on the NYHOPS grid were used because the approach eliminated the need for the extremely time- and CPU-intensive high-resolution year-long simulations for each sea level rise scenario, yet the 68 simulated tidal cycles capture the dynamic combination of "mean" streamflow with tides, water column stratification and sea level rise. The model's streamflow inputs from all 52 freshwater sources into the Hudson (519 sources in total across the entire model domain; Georgas, 2010; Orton et al., 2012) were temporally constant and taken from the operational system for August 22, 2011, a day that exhibited stable, near-mean streamflow values. For example, the streamflow into the tidal Hudson at Troy was  $400 \text{ m}^3/\text{s}$ , whereas the mean at that location in 2010 (used for annual tide simulations in Georgas et al. 2013) was  $455 \text{ m}^3/\text{s}$  and the median was  $340 \text{ m}^3/\text{s}$ . Mean and median values for this location for the period 1989-2013 were 440 and  $330 \text{ m}^3/\text{s}$ , respectively (USGS, 2014), but this value varies over time and for the period 1980-2004 the mean was  $400 \text{ m}^3/\text{s}$  (Orton & Visbeck, 2009). The first two days of the simulation were discarded prior to performing data analysis, as is common due to relatively erratic tide spin-up conditions.

A resulting comparison of observation-based and model-based tide datums is shown in **Figure A3**, and demonstrates a high degree of accuracy. The MHHW biases across all stations averaged +0.06 m, with maximum of 0.14 m at Schodack Island (latitude  $42.504^\circ\text{N}$ ). The biases along the Hudson were fitted with a shape-preserving spline (**Figure A4**) and corrections to the model results applied simply as a function of latitude. For latitudes above Albany ( $42.65^\circ\text{N}$ ), a constant bias value was extrapolated. A spatially-constant bias value of -0.004 m is used for western Long Island Sound, the mean of the Willet's Point and Kings Point values which are both within +/- 0.01 m of that value. Relative to a Hudson River mean present-day depth of about 10 m plus sea level rise scenarios up to 1.83 m (6 ft), these biases will have a negligible effect on the dynamics and resulting MHHW estimates.

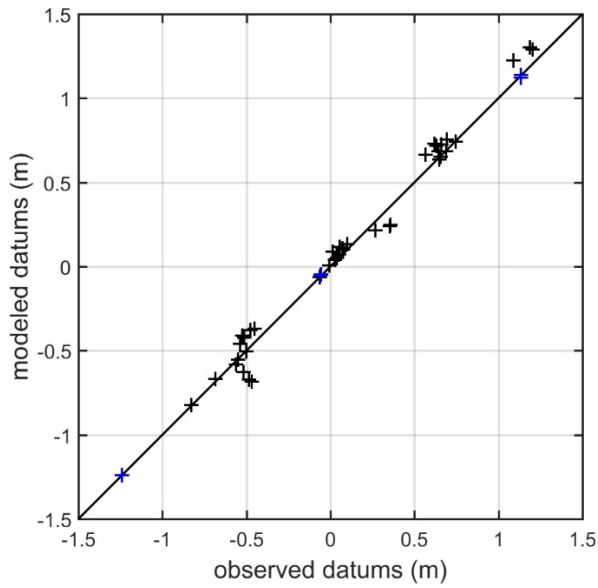


**Figure A3:** Comparison plot for tide datums based on observations versus model, including Mean Lower-Low Water, Mean Sea Level, and MHHW at 13 Hudson River stations from Battery to Albany (black) and Western Long Island Sound stations (blue).

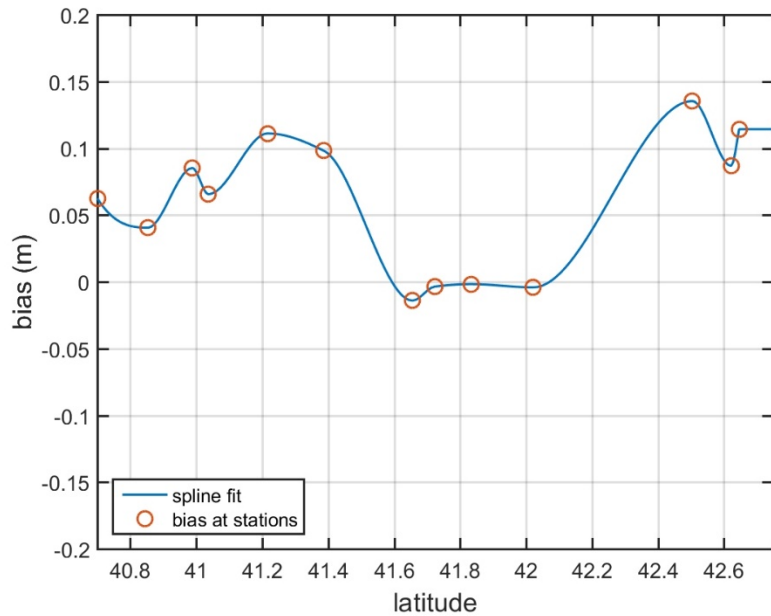


**Figure A4:** Latitudinal dependence of bias in MHHW along the tidal Hudson River, computed as MHHW\_model minus MHHW\_observations, and fitted using a shape-preserving spline. For latitudes above Albany (42.65), a constant bias value was extrapolated.

**Appendix 2. The Variable Framework of the Social Vulnerability Index. The codes used in the last column represent Census variables used for the analysis.**

Dimension of social vulnerability	Sub-dimensions	Variable code	Variable name	Source	Census level	Calculation
Social status	Ethnicity	africanampop	Percent of African American Population	ACS	Block group	$B02001e3 / B02001e1 * 100$
		hisplatpop	Percent of Hispanic/Latino Population	ACS	Block group	$B03002e12 / B03002e1 * 100$
		otherracepop	Percent of people of race other than White, Hispanic, African American	ACS	Block group	$B02001e7 / B02001e1 * 100$
		speakengnotwell	Percent of Population Speaking English Less than very Well	ACS	Block group	$(B16004e7 + B16004e8 + B16004e12 + B16004e13 + B16004e17 + B16004e18 + B16004e22 + B16004e23 + B16004e29 + B16004e30 + B16004e34 + B16004e35 + B16004e39 + B16004e40 + B16004e44 + B16004e45 + B16004e51 + B16004e52 + B16004e56 + B16004e57 + B16004e61 + B16004e62 + B16004e66 + B16004e67) / [B01001e1 - (B01001e27 + B01001e3) * 100] * 100$

Appendix 2 (cont.)

Dimension of social vulnerability	Sub-dimensions	Variable code	Variable name	Source	Census level	Calculation
Social status	Age	popunder5	Percent of Population Under 5	ACS	Block group	$(B01001e3+B01001e27) / B01001e1 * 100$
		popover65	Percent of Population 65 and Over	ACS	Block group	$(B01001e20+B01001e21+B01001e22+B01001e23+B01001e24+B01001e25+B01001e44+B01001e45+B01001e46+B01001e47+B01001e48+B01001e49) / B01001e1 * 100$
		ov65livealone	Percent of People over 65 Living Alone	ACS	Block group	$(B09017e17+B09017e14) / B09017e1 * 100$
		medage	Median age	ACS	Tract	DP5_HC01_VC21
	Gender	femalesingleparhh	Percent of Female Single Parent Households	ACS	Block group	$B09002e15 / B09002e1 * 100$

Appendix 2 (cont.)

Dimension of social vulnerability	Sub-dimensions	Variable code	Variable name	Source	Census level	Calculation
Economic status	Poverty	femalehhpoverty	Percent Female Households Living in Poverty	ACS	Block group	$(B17017e44 + B17017e55) / B17017e31 * 100$
		lvinpoverty	Percent of Population Living in Poverty	ACS	Block group	$B17021e2 / B17021e1 * 100$
		ov65poverty	Percent of Population over 65 Years Old Living in Poverty	ACS	Tract	DP3_HC03_VC173
		childpov	Percent of children living in poverty	ACS	Tract	DP3_HC03_VC168
		snapbenefitshh	Percent of Households receiving SNAP Benefits	ACS	Tract	$DP3\_HC01\_VC99 / DP3\_HC01\_VC74 * 100$

Appendix 2 (cont.)

Dimension of social vulnerability	Sub-dimensions	Variable code	Variable name	Source	Census level	Calculation
Economic status	Poverty	percapincomei	Per Capita Income (inverse)	ACS	Block group	$1/B19301e1$
	Employment	civlabforceunemp	Percent of civilian labor force that is unemployed	ACS	Block group	$B23025e5 / B23025e1 * 100$
		workinghome	Percent of people working from home	ACS	Block group	$B08301e21 / B08301e1 * 100$
		civiltransocc	Percent of Employment in Transportation	ACS	Block group	$(C24010e34 + C24010e70) / C24010e1 * 100$
		civilservocc	Ratio of Employment in Service Industries	ACS	Block group	$(C24010e19 + C24010e55) / C24010e1 * 100$
	Education	pop25nohstdiploma	Ratio of Population Over 25 With No High School Degree	ACS	Block group	$(B15002e10 + B15002e27) / B15002e1 * 100$

Appendix 2 (cont.)

Dimension of social vulnerability	Sub-dimensions	Variable code	Variable name	Source	Census level	Calculation
Economic status	Housing	grossrentmor35	Percent of Housing units with a rent of 35 percent or more	ACS	Tract	DP4_HC03_VC197
		mortggreat35	Percent of Housing units with a mortgage of 35 percent or more	ACS	Tract	DP4_HC03_VC171
		great20units	Percent of Structures with 20 or more Units	ACS	Block group	$(B25024e8 + B25024e9) / B25024e1 * 100$
		singleunit	Ratio of Single Unit Structures	ACS	Block group	$B25024e2 / B25024e1 * 100$

Appendix 2 (cont.)

Dimension of social vulnerability	Sub-dimensions	Variable code	Variable name	Source	Census level	Calculation
Isolation	Social and spatial distance	pubtransp	Percent use of public transportation to the workplace	ACS	Block group	$B08301e10 / B08301e1 * 100$
		travtimemore60	Percent of Population with Travel Time to Work greater than 60 minutes	ACS	Block group	$(B08303e12 + B08303e13) / B08303e1 * 100$
		novehicle	Percent of Housing Units with No Vehicle	ACS	Block group	$(B25044e3 + B25044e10) / B25044e1 * 100$
		nophone	Ratio of Housing Units with No Phone	ACS	Tract	DP4_HC03_VC105
		dist2bus	Distance to bus	ESRI	Block group	
		dist2school	Distance to school	ESRI	Block group	
Health		dist2hosp	Distance to health care centers	ESRI	Block group	

### Appendix 3. Dimensions of Social Vulnerability based on PCA - Block Group Level

Dimension of social vulnerability	Sign Adjustment	Variance explained	Variance (eigenvalues)	Dominant variables (variable codes, in order of importance)	Variable names	Loadings
Deprivation	+	27.96%	8.67	rentoccup	Percent of Renter Occupied Units	0.285
				novehicle	Percent of Housing Units with No Vehicle	0.284
				snapbenefitshh	Percent of Households receiving SNAP Benefits	0.273
				livinpoverty	Percent of Population Living in Poverty	0.267
				childpov	Percent of children living in poverty	0.265
				ov65poverty	Percent of Population over 65 Years Old Living in Poverty	0.211
				femalehhpoverty	Percent Female Households Living in Poverty	0.189
				nophone	Ratio of Housing Units with No Phone	0.164
				percapincomei	Per Capita Income (inverse)	0.142
Isolation	+	7.56%	2.34	pubtransp	Percent use of public transportation to the workplace	0.423
				travtimemore60	Percent of Population with Travel Time to Work greater than 60 minutes	0.323

Appendix 3 (cont.)

Dimension of social vulnerability	Sign Adjustment	Variance explained	Variance (eigenvalues)	Dominant variables (variable codes, in order of importance)	Variable names	Loadings
Race and language		6.35%	1.97	great20units	Percent of Structures with 20 or more Units	0.361
				ov65livealone	Percent of People over 65 Living Alone	0.352
				speakengnotwell	Percent of Population Speaking English Less than very Well	-0.292
				popunder5	Percent of Population Under 5	-0.275
				singleunit	Ratio of Single Unit Structures	-0.246
				medage	Median age	0.226
Family structure and age	+	5.44%	1.68	otherracepop	Percent of people of race other than White, Hispanic, African American	0.350
				hisplatpop	Percent of Hispanic/Latino Population	0.337
				civiltransocc	Percent of Employment in Transportation	0.318
				civilservocc	Ratio of Employment in Service Industries	0.286
				dist2hosp	Distance to health care centers	0.204
				dist2school	Distance to school	0.158

Appendix 3 (cont.)

Dimension of social vulnerability	Sign Adjustment	Variance explained	Variance (eigenvalues)	Dominant variables (variable codes, in order of importance)	Variable names	Loadings
Dependency		4.13%	1.28	popover65	Percent of Population 65 and Over	-0.438
				pop25nohsdiploma	Ratio of Population Over 25 With No High School Degree	-0.354
				mortggreat35	Percent of Housing units with a mortgage: of 35 percent or more	-0.342
				africanampop	Percent of African American Population	0.316
				civlabforceunemp	Percent of civilian labor force that is unemployed	0.293
				femalesingleparhh	Percent of Female Single Parent Households	0.253

### Appendix 4. Dimensions of Social Vulnerability based on PCA - Municipal Level

Dimension of social vulnerability	Sign Adjustment	Variance explained	Variance (eigenvalues)	Dominant variables (variable codes, in order of importance)	Variable names	Loadings
Deprivation	-	31.55%	9.78	novehicle	Percent of Housing Units with No Vehicle	-0.287
				rentoccup	Percent of Renter Occupied Units	-0.277
				livinpoverty	Percent of Population Living in Poverty	-0.244
				snapbenefitshh	Percent of Households receiving SNAP Benefits	-0.241
				femalesingleparhh	Percent of Female Single Parent Households	-0.240
				childpov	Percent of children living in poverty	-0.237
				africanampop	Percent of African American Population	-0.236
				ov65poverty	Percent of Population over 65 Years Old Living in Poverty	-0.202
				nophone	Ratio of Housing Units with No Phone	-0.169
				femalehhpoverty	Percent Female Households Living in Poverty	-0.166

Appendix 4 (cont.)

Dimension of social vulnerability	Sign Adjustment	Variance explained	Variance (eigenvalues)	Dominant variables (variable codes, in order of importance)	Variable names	Loadings
Isolation	+	14.94%	4.63	pubtransp	Percent use of public transportation to the workplace	0.323
				travtimemore60	Percent of Population with Travel Time to Work greater than 60 minutes	0.286
				hisplatpop	Percent of Hispanic/Latino Population	0.226
				otherracepop	Percent of people of race other than White, Hispanic, African American	0.222
				speakengnotwell	Percent of Population Speaking English Less than very Well	0.187
				percapincomei	Per Capita Income (inverse)	-0.303
Housing and Age	+	6.10%	1.89	grossrentmor35	Percent of Housing units with a rent of 35 percent or more	0.346
				popover65	Percent of Population 65 and Over	0.339
				medage	Median age	0.302
				workinghome	Percent of people working from home	0.290
				mortggreat35	Percent of Housing units with a mortgage: of 35 percent or more	0.170

Appendix 4 (cont.)

Dimension of social vulnerability	Sign Adjustment	Variance explained	Variance (eigenvalues)	Dominant variables (variable codes, in order of importance)	Variable names	Loadings
Dependency		5.40%	1.67	pop25nohdsdiploma	Ratio of Population Over 25 With No High School Degree	0.309
				ov65livealone	Percent of People over 65 Living Alone	-0.309
				great20units	Percent of Structures with 20 or more Units	-0.300
				civiltransocc	Percent of Employment in Transportation	0.255
				popunder5	Percent of Population Under 5	0.224
				singleunit	Ratio of Single Unit Structures	0.216
				civilservocc	Ratio of Employment in Service Industries	0.170
				civlabforceunemp	Percent of civilian labor force that is unemployed	0.167
Remoteness	-	5.01%	1.55	dist2hosp	Distance to health care centers	-0.610
				dist2school	Distance to school	-0.528